Applied Catalysis B: Environmental 189 (2016) 19–25

Contents lists available at ScienceDirect

Applied Catalysis B: Environmental

journal homepage: www.elsevier.com/locate/apcatb

Acidity-regulation for enhancing the stability of Ni/HZSM-5 catalyst for valeric biofuel production

Peng Sun [1], Guang Gao [1], Zelun Zhao, Chungu Xia, Fuwei Li *

State Key Laboratory for Oxo Synthesis and Selective Oxidation, Suzhou Research Institute of LICP, Lanzhou Institute of Chemical Physics (LICP), Chinese Academy of Sciences, Lanzhou 730000, PR China

ARTICLE INFO

Article history:
Received 7 December 2015
Received in revised form 1 February 2016
Accepted 9 February 2016
Available online 11 February 2016

Keywords:
Deactivation
Stability
Levulinic acid
Valerate esters

ABSTRACT

Valerate esters as a new class of cellulosic transportation fuels showed great industrial prospect. Here we developed a non-noble Ni/HZSM-5 bifunctional catalyst with excellent stability for the cascade transformation of levulinic acid to valerate esters. The acidity-regulation of Ni/HZSM-5 catalyst by potassium addition decreased the strong acidity, meanwhile tuned the proportion of Brönsted acidity/Lewis acidity. Coke analysis indicated that acidity-regulation by potassium addition changed the heavier coke component (alkylated poly-aromatics) to the lighter one (alkylated mono-aromatics), thus effectively prolonged the lifetime of Ni/HZSM-5 catalyst in fixed-bed reactor. The relationship of the nature of coke deposits and the acidity-regulation of catalysts could contribute to intensively understand the catalyst deactivation and the choice of stable catalyst for upgrading of biomass and its platform molecules.

1. Introduction

Biomass and its derivatives suffer from abundant functionality that makes them easy to polymerize at high temperature, finally causes the catalyst fast deactivation. At this point, the stability of the catalyst is necessary for the transformation of biomass and its derivatives to chemicals and liquid fuels [1]. Levulinic acid (LA) is such a prominent bio-derived platform molecule with a carbonyl and a carboxyl group [2]. LA can be converted to valerate esters via tandem reaction (Scheme 1), including hydrogenation to valerolactone (GVL), ring-opening to pentenoic acid, hydrogenation to valeric acid (VA) and esterification to valerate esters. Valerate esters with promising potential for mixing with gasoline and diesel components have been recognized as a new class of cellulose-derived fuels, called "valeric biofuels" [3,4]. Its industrial prospect has been exhibited via a road trial of 250,000 km by Shell Lab in 2010 [5]. They also noted that the yield of VA from GVL over Pt/HZSM-5/SiO_2 catalyst dropped from initial 70% to 35% with time on stream (25 h), signifying the catalyst deactivation occurred during this transformation. However, the catalyst deactivation was not further investigated.

Currently, most studies focus on improving the yield of VA and/or its esters with solid acid supported noble metal catalyst (Ru/HZSM-5 [6], Ru/SBA-SO_3H [7], Pd/Nb_2O_5 [8–11], Pd/HY [12,13]) and non-noble metal catalyst Co@HZSM-5 [14]. Few study concerns the long-term stability of catalyst during this tandem transformation. Because of the high cost of catalyst precursors (e.g., noble metal) and complicated catalyst preparation, it is desirable to develop a cost-effective and stable catalyst to boost the industrial manufacture of valerate esters.

As another cheap candidate to noble metal, nickel displays good catalytic performance in hydrogenation [15] and hydrogenolysis reactions [16], but its application in the transformation of LA into VA and/or its esters has not been discovered. From the economical point, nickel is more earth-abundant and cheaper than noble metals. For example, Pt is the common metal used in the production of VA. The price of Pt (28.8 $/g) is 3381 times of the price of metal Ni (8518 $/t) based on the data of London Metal Exchange. Herein, HZSM-5 supported Ni catalyst prepared by simple impregnation has been firstly employed in the catalytic cascade conversion of LA into ethyl valerate (EV) over fixed-bed reactor.

In view of the ring-opening of GVL to pentenoic acid needs a high free energy change ($\Delta G = +1.5$ kJ mol^{-1} and +25 kJ mol^{-1} in methanol and H_2O, respectively) [17], the acidity of catalyst should be strong enough to catalyze the ring-opening of GVL. At the same time, suppression of the coke formation needs weaken the acid strength of the catalytic sites [18–20]. Therefore, to balance the need of acid-catalyzed GVL ring-opening reaction and the inhibi-

* Corresponding author.
E-mail address: fuweili@licp.cas.cn (F. Li).
[1] These authors contributed equally.

http://dx.doi.org/10.1016/j.apcatb.2016.02.026
0926-3373/

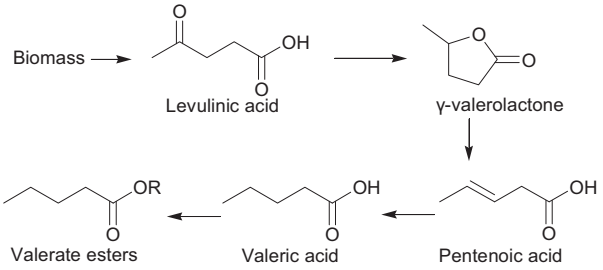

Scheme 1. Reaction pathways for production of valerate esters from biomass.

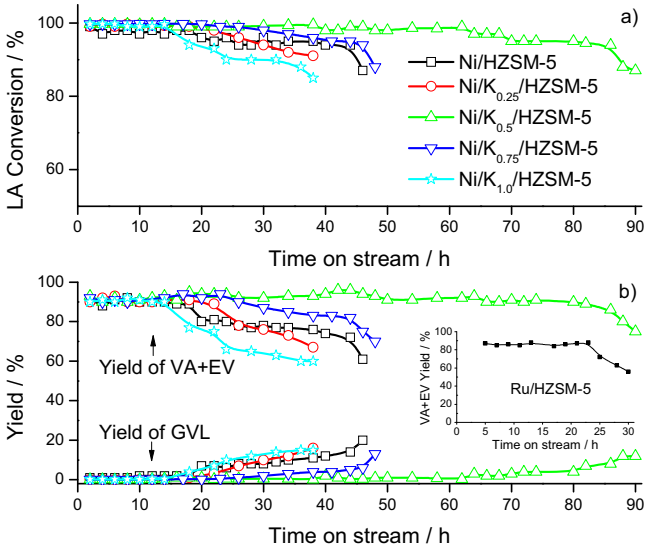

Fig. 1. (a) LA conversion and (b) products yields over Ni/HZSM-5 and Ni/K_x/HZSM-5 catalysts as a function of TOS. (Inset is the yield of VA/EV versus TOS over Ru/HZSM-5).

tion of coke formation, the regulation of support acidity should be necessary to develop an efficient and stable bifunctional catalyst. Generally, preparation of zeolites catalysts with lower acidity could be realized by (a) controlling the Si/Al ratio [21], pH value and calcinations temperature during synthesis [22]; (b) introducing alkali or alkaline-earth metals by ionic-exchange or impregnation [20], steaming treatment [23], aging in hot water [24], and deposition of SiO_2 shell [25] during post-synthesis. Among these methods, introduction of alkali metal is a simple and efficient method to regulate the acidity of zeolites. In this context, we investigated the influence of potassium addition on the acidity, catalytic performance and stability of HZSM-5 supported Ni catalyst for the tandem transformation of LA to VA/EV, and illustrated the correlation between the acidity-regulation of catalyst and the nature of coke deposit.

2. Experimental

2.1. Catalyst preparation

Ni supported on HZSM-5 zeolite (noted as Ni/HZSM-5) was prepared by impregnation method with metal content of 10 wt%. Commercial HZSM-5 zeolite (Si/Al = 38) was added in an aqueous solution of $Ni(NO_3)_2{\cdot}6H_2O$ and stirred for 24 h. After drying, the solid was calcined at 500 °C for 5 h and reduced at 450 °C for 4 h.

HZSM-5 supports with various potassium content from 0.25 to 1.0 wt% were prepared by similar impregnation method with KNO_3 as precursor. The as-prepared supports were calcined at 500 °C for 5 h. Finally, Ni supported on potassium modified HZSM-5 (donated as Ni/K_x/HZSM-5) was prepared with the same routine as Ni/HZSM-5, where *x* represented the corresponding potassium content (wt%).

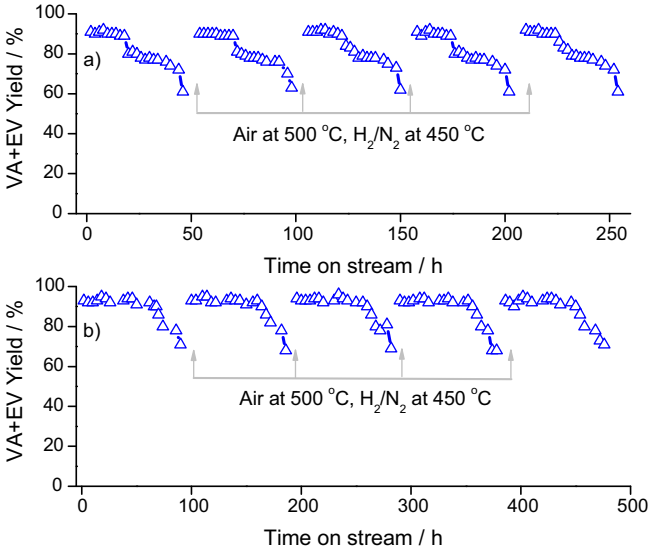

Fig. 2. Long-term operation over (a) Ni/HZSM-5 and (b) Ni/$K_{0.5}$/HZSM-5 with multiple regenerations by calcination and H_2 reduction.

2.2. Catalysts characterization

The morphology of supported Ni was observed by transmission electron microscopy (TEM) with JEM 1200 EX (JEOL) and FEI Tecnai G2 F20 S-Twin electron microscope.

The metal leaching was measured by inductively coupled plasma atomic emission spectroscopy (ICP-AES) using a Perkin-Elmer OPTIMA 3300 DV spectrometer (Norwalk, CT, U.S.A.).

The acidity of fresh catalyst was measured by NH_3 temperature-programmed desorption (NH_3-TPD) with a XIANQUAN tp-5080 instrument (Tianjin, China) using the standard routine.

The Brönsted and Lewis acidities of fresh and spent catalysts were estimated by in situ pyridine adsorption with FT-IR spectrometer (Bruker, Tensor 27). The catalysts were sheeted and vacuumed in the in situ IR cell (1×10^{-3} Pa) at 200 °C for 2 h, and then cooled to 40 °C to adsorb pyridine.

BET area of sample was measured by N_2 physisorption with a Micromeritics TriStar II 3020 analyzer. Before measurement, the catalysts were treated at 250 °C for 4 h under N_2 to eliminate impurities.

The coke content on spent catalyst was determined by thermogravimetric analysis (TGA) using a Mettler-Toledo TGA/DSC 1 instrument. The coked samples were heated from room temperature to 800 °C by a rate of 10 °C min^{-1} under air (50 mL min^{-1}).

Temperature-programmed oxidation (TPO) was conducted on Micromeritics AutoChem II 2920 with an AMETEK/DYCOR MS detector. The coked samples were pretreated at 150 °C under He for 30 min, then cooled to room temperature and heated to 600 °C at rate of 10 °C min^{-1} under 2% O_2/He. The signal of CO_2 was monitored by MS detector.

Element analysis of freed coke deposit was achieved on Element Vario EL instrument. Freed coke was obtained by complete dissolution of deactivated catalyst in hydrofluoric acid solution.

The morphology of freed coke deposit was observed using a field-emission scanning electron microscope (FEI, S4800).

FT-IR spectroscopy of sample was attained using a Nicolet 6700 spectrometer. The sample was pelletized with KBr.

Temperature-programmed desorption mass spectrum (TPD-MS) was conducted on Micromeritics AutoChem II 2920 with an

AMETEK/DYCOR MS detector. The coked catalysts were charged in U-shaped tube and heated from 100 to 500 °C (10 °C min^{-1}) under N_2; the desorbed species were detected by MS.

2.3. Catalytic reaction

The continuous-flow experiments were performed with a tubular stainless steel reactor (8 mm inner diameter) at 240 °C and 3 MPa H_2. The catalyst (2 g) was charged between two quartz wool plugs, above which was 2 mL quartz sand. Firstly, the catalyst was reduced at 450 °C under H_2, and cooled to 240 °C, and then the feedstock (16.7 wt% of LA in ethanol) was pumped into the reactor with weight hour space velocity (WHSV) of 2.96 h^{-1}. The products were analyzed by gas chromatograph (Agilent 7890A) and GC-MS (Agilent 5975C/7890A). The deactivated catalyst was regenerated by calcination in air at 500 °C for 3 h and reduction at 450 °C under H_2.

3. Results and discussion

3.1. Catalytic performance

The catalytic performances of Ni/HZSM-5 and Ni/K_x/HZSM-5 catalysts are presented in Fig. 1. Complete LA conversions (Fig. 1a) were achieved on both parent and potassium modified samples at 2 h time on stream (TOS), and kept stable for about 20 h, then declined with varying degrees over different samples with TOS, except for Ni/$K_{0.5}$/HZSM-5, on which full LA conversion was kept for 80 h. To accurately compare the stability of the parent and potassium modified catalysts, the deactivation parameter D [26,27] ($D = [X_0 - X_t] \times 100\%/X_0$, where X_0 was the initial LA conversion and X_t was the LA conversion at TOS of 38 h) was employed to evaluate the deactivation rate. The calculated D values of Ni/HZSM-5, Ni/$K_{0.25}$/HZSM-5, Ni/$K_{0.5}$/HZSM-5, Ni/$K_{0.75}$/HZSM-5, Ni/$K_{1.0}$/HZSM-5 catalysts were 5.0, 8.0, 0.1, 3.0 and 14.0%, respectively. A smaller value for D implied a longer catalyst lifetime. Compared with the parent Ni/HZSM-5 and other potassium modified samples, Ni/$K_{0.5}$/HZSM-5 sample exhibited the smallest D value and correspondingly obtained the longest catalyst lifetime.

As shown in Fig. 1b, the yield of VA/EV over parent Ni/HZSM-5 catalyst was about 90% at TOS of 2 h and reached a steady state within 18 h followed by a slow fading, which was comparative with that of HZSM-5 supported noble Ru catalyst (Inset). After 38 h of TOS, the VA/EV yields over Ni/HZSM-5, Ni/$K_{0.25}$/HZSM-5, Ni/$K_{0.75}$/HZSM-5 and Ni/$K_{1.0}$/HZSM-5 declined from initial 90% to 75%, 67%, 83% and 60%, respectively. Meanwhile, as the VA/EV yields declined with TOS, the GVL yield gradually increased over these catalysts, suggesting the acid-catalyzed ring-opening of GVL was blocked. Contrarily, Ni/$K_{0.5}$/HZSM-5 catalyst held >90% yield of VA/EV until 80 h. Based on the above result, it could be concluded that when potassium addition was 0.5 wt%, the catalyst exhibited the lowest deactivation rate and the corresponding catalyst lifetime was significantly extended to 80 h, which was about four times the lifetime of parent Ni/HZSM-5 (18 h).

To explore the origin of catalyst deactivation during long-term operation was whether from metal sintering/leaching or coke deposition, the deactivated Ni/HZSM-5 and Ni/$K_{0.5}$/HZSM-5 catalysts were regenerated by calcinations under air flow at 500 °C for 3 h to remove the coke deposition and further reduced at 450 °C under H_2, and the regenerated catalysts were used for the cascade conversion of LA again. Generally, if deactivation was caused by coke deposition, the catalytic performance of deactivated catalyst would be recovered after the carbon species was burned by calcinations. However, metal sintering/leaching would result in decrease of the number of exposed active sites/loss of active sites [1], therefore deactivation caused by metal sintering/leaching could not be recovered by calcinations [28]. As depicted in Fig. 2, both deactivated Ni/HZSM-5 and Ni/$K_{0.5}$/HZSM-5 catalysts could be fully recovered for five runs by regeneration, indicating the deactivation of catalyst was caused by the coke deposition rather than metal sintering/leaching. To confirm metal sintering/leaching was not occurred, the Ni particles were characterized in the following catalyst characterization.

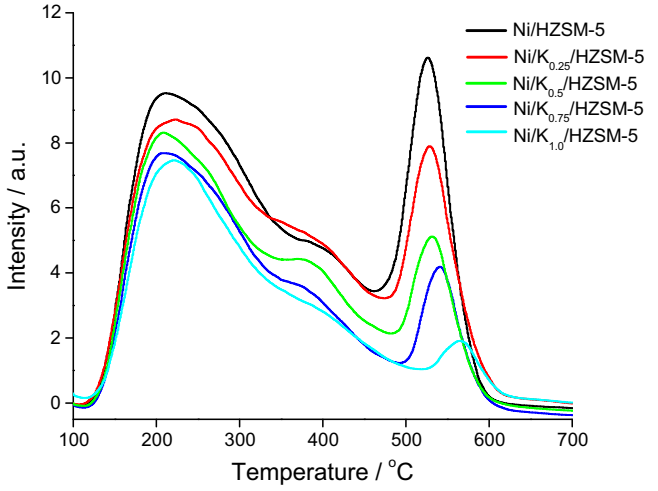

Fig. 3. NH_3-TPD patterns of Ni/HZSM-5 and Ni/K_x/HZSM-5 catalysts.

3.2. Characterization of fresh and coked catalyst

Next, we focus on illustrate the relationship of potassium addition to catalyst physico-chemical properties. Initially, the morphology of Ni particles was observed by TEM. As depicted in Fig. S1a, the Ni particles with average size of 38 nm were uniformly distributed on HZSM-5 support. After addition of potassium, the Ni particles were not influenced (Fig. S1b). Besides, the 48 h coked Ni/HZSM-5 (Fig. S1c) and 90 h coked Ni/$K_{0.5}$/HZSM-5 (Fig. S1d) presented Ni size similar to their fresh counterparts, respectively; indicating Ni particles were not sintered during long-term reaction. ICP-AES measurement verified that Ni leaching was not found in the reaction solution. TEM and ICP-AES results further confirmed that the deactivation of catalyst was not caused by sintering/leaching of metal Ni. The acidity of Ni/HZSM-5 regulated by potassium addition was characterized by NH_3-TPD. As shown in Fig. 3, two desorption peaks appeared over Ni/HZSM-5, which could be assigned to the weak acid sites (110–450 °C) and the strong acid sites (450–600 °C), respectively. The area of desorption peaks could reflect the acid amounts. After potassium addition, the acid amounts, especially the strong acid amounts on Ni/K_x/HZSM-5, significantly decreased as the enhancement of potassium content. The amount ratio of weak acid to strong acid (noted as W/S in Table 1) was calculated by integrated area of desorption peak in NH_3-TPD profiles. The ratio of W/S was raised as the increase in potassium loading, demonstrating the potassium addition could effectively regulate the acid amount of Ni/HZSM-5. Considering the strong acid sites facilitated the dehydrogenation and condensation reactions for coke formation, consequently, the decline of strong acid sites in the ratio of W/S could alleviate the formation of coke and bring the improvement of catalyst lifetime from 18 h (Ni/HZSM-5) to 80 h (Ni/$K_{0.5}$/HZSM-5) in Fig. 1b. However, potassium addition with excessive loading (Ni/$K_{1.0}$/HZSM-5) led to the drop in catalyst lifetime (14 h, Fig. 1b), which might be caused by the massive decrease in the acid amounts of the catalyst resulted from pore blockage by excess potassium [29].

Table 1
Physico-chemical properties of Ni/HZSM-5 and Ni/K_x/HZSM-5 catalysts.

Sample	W/S[a]	Acidity[b]/μmol g^{-1}			S_{BET}[c]/m^2 g^{-1}	H/C[d] ratio
		B	L	B/L		
Ni/HZSM-5	4.0	478	86	5.5	230	–
Ni/$K_{0.25}$/HZSM-5	5.0	402	79	5.1	214	–
Ni/$K_{0.5}$/HZSM-5	5.9	280	73	3.8	224	–
Ni/$K_{0.75}$/HZSM-5	7.6	264	63	4.2	211	–
Ni/$K_{1.0}$/HZSM-5	19	200	44	4.5	216	–
Ni/HZSM-5, spent 1 h	–	–	–	–	5.9	1.3
Ni/$K_{0.5}$/HZSM-5, spent 1 h	–	53	15	3.5	50.3	1.5

[a] Weak acid/strong acid, determined by integrated area of desorption peak in NH_3-TPD profiles.
[b] Brönsted and Lewis acidity measured by pyridine adsorption at 400 °C (fresh catalyst) and 150 °C (coked catalyst).
[c] Measured by N_2 adsorption-desorption.
[d] Determined by element analysis of freed coke.

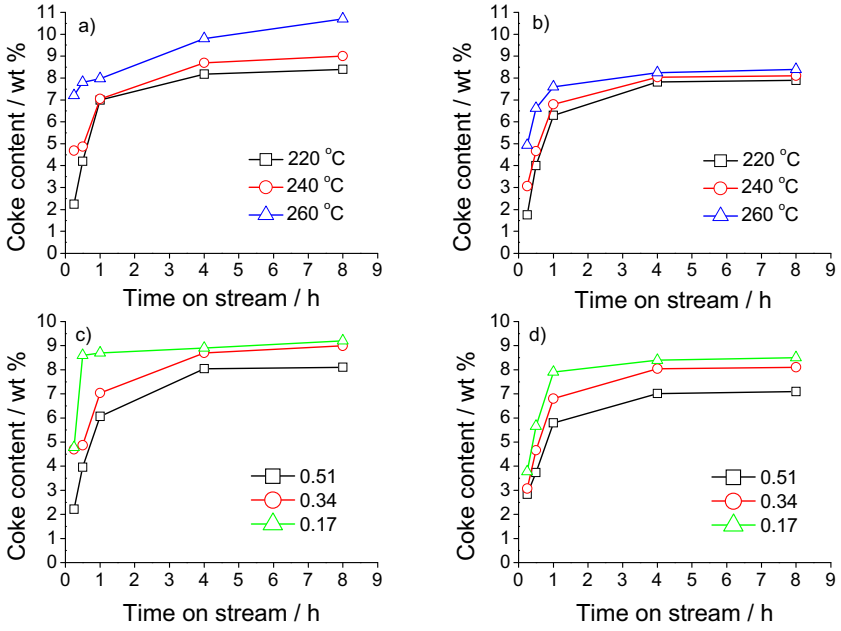

Fig. 4. Evolution of coke content with TOS at different temperature over (a) Ni/HZSM-5 and (b) Ni/$K_{0.5}$/HZSM-5; at different contact time[a] over (c) Ni/HZSM-5 and (d) Ni/$K_{0.5}$/HZSM-5. [a] in units of (g of catalyst) h (g of LA)$^{-1}$.

Pyridine adsorption FT-IR spectroscopy was employed to characterize the Brönsted and Lewis acidities of the fresh samples (Table 1). Both Brönsted and Lewis acidities gradually decreased with increase of potassium content. However, the B/L ratio dropped firstly and then rose later with potassium content from 0 to 1.0 wt%; it reached to the minimum at the potassium content of 0.5 wt%. Combining this with the longest lifetime of Ni/$K_{0.5}$/HZSM-5 catalyst shown in Fig. 1, it could be deduced that proper proportion of B/L was advantageous to realize the long catalyst lifetime. NH_3-TPD and pyridine adsorption FT-IR results indicated that modification of potassium on the Ni/HZSM-5 catalyst weakened the strong acidic sites, meanwhile changed the proportion of B/L, which consequently improved the catalytic stability of Ni/HZSM-5 for the cascade conversion of LA.

To investigate the influence of coke deposit on active acid sites, the acidities of spent Ni/HZSM-5 and Ni/$K_{0.5}$/HZSM-5 were also characterized by IR spectra of adsorbed pyridine (Table 1). After only 1 h TOS, the Ni/HZSM-5 already lost total Brönsted and Lewis acidities; Ni/$K_{0.5}$/HZSM-5 showed 81% loss of acidities, indicating the coke deposit caused a fast loss of acid sites. BET area of fresh and coked samples measured by N_2 adsorption-desorption is also listed in Table 1. For fresh sample, potassium addition had a little impact on BET area, but after 1 h TOS reaction, Ni/HZSM-5 and Ni/$K_{0.5}$/HZSM-5 lost 97% and 77% of microporosity, respectively. Although Ni/HZSM-5 lost almost total acid sites and microporosity at 1 h TOS, it still achieved 100% LA conversion and 90% VA/EV yield until 18 h. The similar phenomenon was also observed in HZSM-5 zeolite catalyzed conversion of ethanol to hydrocarbon, where the high catalytic performance of catalyst after loss of acidity and microporosity was ascribed to the presence of active radical species among the carbonaceous deposits [30]. In our case, Ni/$K_{0.5}$/HZSM-5 lost major acid sites and microporosity at 1 h TOS, but it held 100% LA conversion and 90% VA/EV yield for 80 h, suggesting the nature of carbonaceous deposits was significantly changed by potassium addition. Next, we concentrated on the coke analysis to explore the nature of carbonaceous deposits formed on Ni/HZSM-5 and Ni/$K_{0.5}$/HZSM-5.

3.3. Coke analysis

Considering the dehydration of ethanol may occur on HZSM-5 zeolites, blank experiment (100% ethanol as feedstock) was performed to exclude the possibility of coke from ethanol. As shown in Fig. S2, under our reaction conditions, the coke caused by ethanol was negligible, thus ensuring the coke deposits was only from LA conversion.

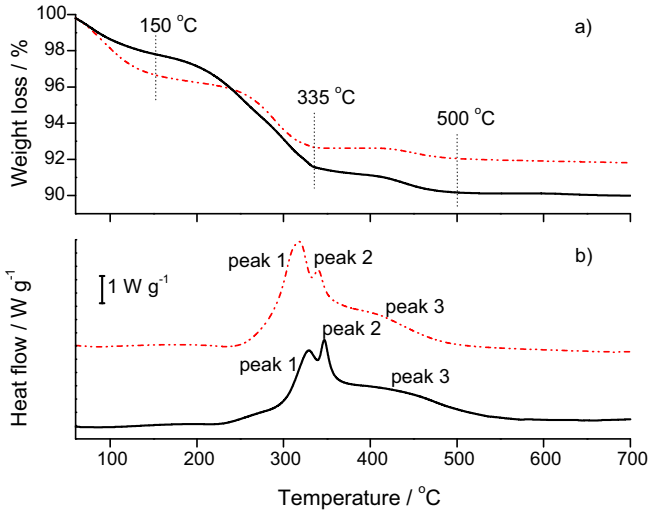

Fig. 5. (a) TG profiles and (b) heat flow profiles of spent Ni/HZSM-5 with 48 h TOS (solid line) and Ni/$K_{0.5}$/HZSM-5 with 90 h TOS (dashed line).

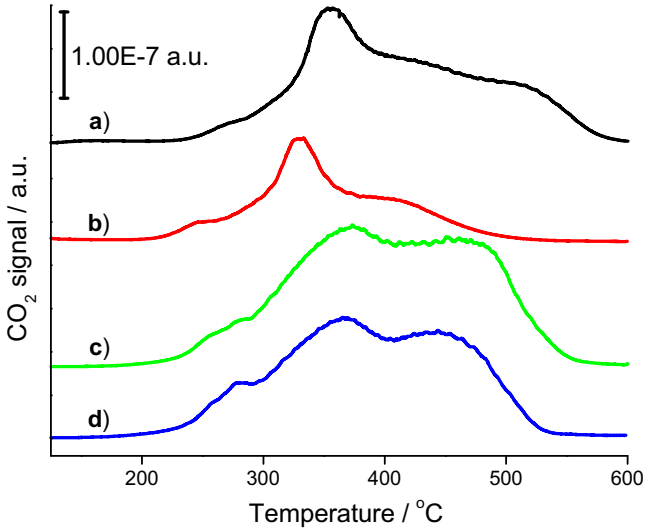

Fig. 6. TPO curves of 1 h coked (a) Ni/HZSM-5 and (b) Ni/$K_{0.5}$/HZSM-5, (c) 48 h coked Ni/HZSM-5, (d) 90 h coked Ni/$K_{0.5}$/HZSM-5.

To investigate the effect of acidity-regulation on coke formation, the evolution of deposited coke content with TOS, in wt% referred to catalyst was shown at different temperature (Fig. 4a and b). For both Ni/HZSM-5 and Ni/$K_{0.5}$/HZSM-5 samples, the near vertical slopes at 0 to 1 h TOS was observed, demonstrating that the coke generated very rapidly in the initial stage of reaction, and tended to stable after 4 h TOS. Higher temperature resulted in more coke deposition, indicating that higher temperature favored the coke-forming reaction. The coke content on Ni/$K_{0.5}$/HZSM-5 was less than that formed on Ni/HZSM-5 under the same conditions, especially at higher temperature, suggesting that acidity-regulation by proper addition of potassium could effectively suppress the formation of coke.

The influence of acidity-regulation was also reflected by coke content at various contact time. As shown in Fig. 4c and d, coke content decreased with increasing contact time, indicating that coke deposit preferentially accumulated on the top access of the fixed-bed reactor and decreased along the perpendicular direction [31], which meant the feedstock, LA rather than products, caused the formation of coke. Also, the Ni/$K_{0.5}$/HZSM-5 sample obtained less coke content than Ni/HZSM-5.

The weight loss of spent Ni/HZSM-5 and Ni/$K_{0.5}$/HZSM-5 catalyst was determined by TGA (Fig. 5a). For both samples, three weight loss stages were observed at 50–150 °C, 150–335 °C and 335–500 °C. The first weight loss at 50–150 °C could be ascribed to desorption of adsorbed H_2O on catalyst. The second and third weight loss corresponded to coke combustion on catalyst [32]. Coked Ni/HZSM-5 with 48 h TOS lost 9.6% of original weight, while the weight loss of Ni/$K_{0.5}$/HZSM-5 with 90 h TOS was 8.2%. The Ni/$K_{0.5}$/HZSM-5 catalyst with longer TOS obtained less coke deposit, suggesting a better anti-coking ability.

During the combustion of coke on catalyst, heat was released synchronously, which could provide useful information for understand the nature of the coke components. As presented in Fig. 5b, three peaks of the heat flow signal could be attributed to different coke species [32–35]. Peaks 1 and 2 were sharp and close to each other in the range of 240–380 °C, correlating with the second weight loss in TGA. Peak 3 was broad in the range of 380–500 °C, corresponding to the third weight loss in TGA. Comparing with coked Ni/$K_{0.5}$/HZSM-5, the position of three peaks over coked Ni/HZSM-5 moved to higher temperature, suggesting the coke on Ni/HZSM-5 was more heavily condensed coke species.

In addition to TGA, TPO was performed to further analyze the coke on spent Ni/HZSM-5 and Ni/$K_{0.5}$/HZSM-5 catalysts. During TPO, CO_2 was released along with coke burning. As displayed in Fig. 6, the CO_2 peak of 1 h coked Ni/HZSM-5 appeared at higher temperature (355 °C) than that of 1 h coked Ni/$K_{0.5}$/HZSM-5 (330 °C), indicating that the coke formed on Ni/HZSM-5 was harder to burn since the initial stage of reaction. An obvious shift of CO_2 peak to higher temperature and a distinct increase of intensity were observed on 48 h coked Ni/HZSM-5 and 90 h coked Ni/$K_{0.5}$/HZSM-5, compared with their 1 h coked counterparts, respectively. This demonstrated that long-term reaction not only made the coke species heavier but also led to weight increment of coke species. Consistent with the result of heat flow, three CO_2 peaks were observed in the range of 240–550 °C for 48 h coked Ni/HZSM-5 and 90 h coked Ni/$K_{0.5}$/HZSM-5 samples, suggesting different coke species; and the three CO_2 peaks over 48 h coked Ni/HZSM-5 shifted to higher temperature than 90 h coked Ni/$K_{0.5}$/HZSM-5, further confirming that more heavily condensed coke species were formed on Ni/HZSM-5.

The hydrogen content in coke deposits could also reflect the constituents of coke species. The H/C ratios of coke species were measured by element analysis after the coke deposits were released by dissolving the zeolites in HF. The H/C ratios of coke species from spent Ni/HZSM-5 and Ni/$K_{0.5}$/HZSM-5 samples were calculated to be 1.3 and 1.5 (Table 1), respectively, demonstrating a lighter coke composition in Ni/$K_{0.5}$/HZSM-5 sample. Hence, it could be concluded from the results of TGA, TPO and H/C ratios that the Ni/$K_{0.5}$/HZSM-5 catalyst achieved not only a less coke content but also a lighter coke constituent than Ni/HZSM-5, which meant that acidity-regulation by potassium addition could effectively alleviate the formation of heavy coke species.

The morphology of freed carbon deposits were observed by SEM. As shown in Fig. 7, both coke deposits from Ni/HZSM-5 and Ni/$K_{0.5}$/HZSM-5 presented the shape of carbon balls with uniform size. The difference was that the size of carbon ball (1 μm) formed on 48 h Ni/HZSM-5 was bigger than that on 90 h Ni/$K_{0.5}$/HZSM-5 (0.5 μm), suggesting acidity-regulation by potassium addition surely inhibited the formation of carbon deposits.

Next we focus on study the nature of coke formed on potassium modified and parent catalyts by IR analysis (Fig. 8). 1 h coked Ni/HZSM-5 and Ni/$K_{0.5}$/HZSM-5 exhibited similar vibration bands but different intensities. The vibration bands in the range of 1500–1640 cm^{-1} and 1350–1470 cm^{-1} were ascribed to the aromatic rings and the alkyl branches of the aromatics, respectively [36]. The IR results suggested that the components of carbon

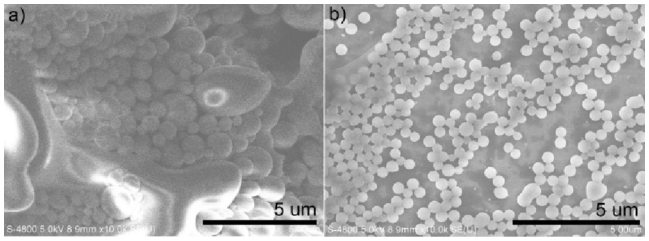

Fig. 7. SEM images of freed carbon deposits. (a) 48 h coked Ni/HZSM-5 and (b) 90 h coked Ni/$K_{0.5}$/HZSM-5 catalyst.

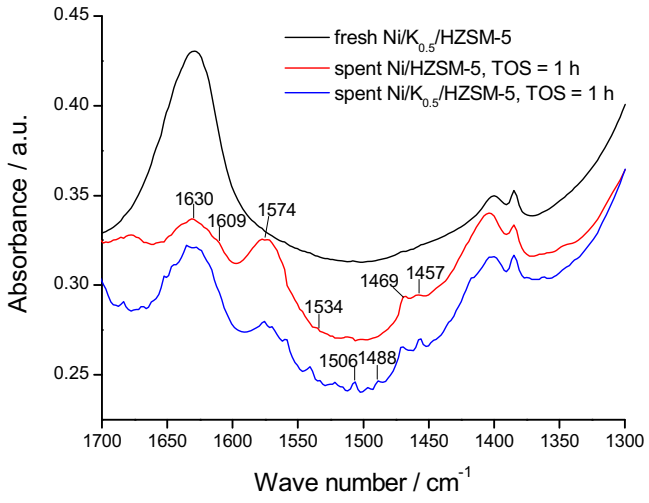

Fig. 8. IR spectra for the 1 h coked Ni/HZSM-5 and Ni/$K_{0.5}$/HZSM-5.

deposits on Ni/HZSM-5 and Ni/$K_{0.5}$/HZSM-5 were alkylated aromatic molecules.

TPD-MS measurements were conducted to further identify the nature of carbonaceous compounds. The spent samples were placed in a U-shaped reactor and heated under N_2 carrier; the desorbed species were monitored by MS. Although the upper limit that could be detected by this MS detector was 200 *m*/*z*, the desorbed species could reveal the nature of coke deposits to a great degree. As displayed as Fig. 9a, the desorbed species from 1 h coked Ni/HZSM-5 were condensed, alkylated, polycyclic aromatic compounds. These giant molecules might block the pores, and hamper the reactants to enter the inside of the channel or the products to escape. Contrarily, mainly alkylated mono-aromatics were found for the Ni/$K_{0.5}$/HZSM-5 (Fig. 9b). Based on the results of IR analysis and TPD-MS, it could be deduced that the carbon deposits formed on Ni/$K_{0.5}$/HZSM-5 and Ni/HZSM-5 consisted of alkylated mono-aromatics and poly-aromatics, respectively. Therefore, acidity-regulation by appropriate potassium addition (Ni/$K_{0.5}$/HZSM-5) could obtain lighter coke component, thus contribute to a longer catalyst lifetime for the cascade conversion of LA into VA/EV.

4. Conclusions

Fast deactivation was observed on Ni/HZSM-5 catalyzed conversion of LA to VA/EV after TOS of 20 h. Addition of potassium in Ni/HZSM-5 catalyst decreased the strong acidity, meanwhile tuned the ratio of Brönsted acidity/Lewis acidity. Acidity-regulation by potassium addition could decrease the coke content under various reaction temperature and contact time. Coke deposit evolution under various contact time indicated the feedstock, LA rather than products, caused the formation of coke. Coke analysis indicated that acidity-regulation by potassium addition changed the heavier coke component (alkylated poly-aromatics) to the lighter one (alkylated mono-aromatics), thus effectively prolonged the lifetime of Ni/HZSM-5 catalyst during long-term operation. The optimum catalyst was Ni/$K_{0.5}$/HZSM-5, over which the longest lifetime (80 h) could be achieved. The relationship of the nature of coke deposits and the acidity-regulation of catalysts could contribute to intensively understand the catalyst deactivation and the choice of stable catalyst for upgrading of biomass and its platform molecules.

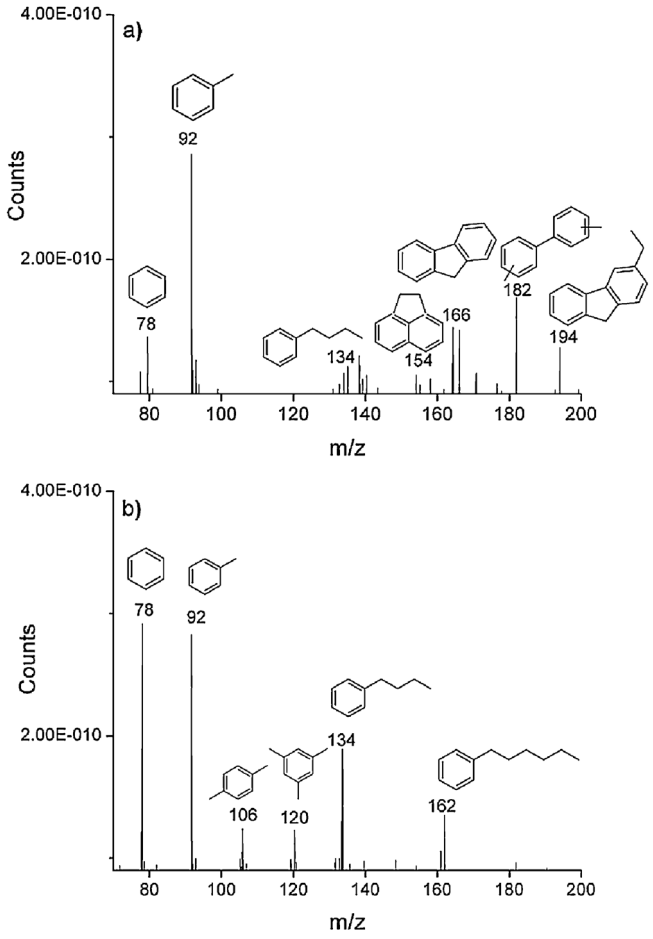

Fig. 9. MS analysis of desorbed components from 1 h coked (a) Ni/HZSM-5 and (b) Ni/$K_{0.5}$/HZSM-5 catalyst.

Acknowledgments

This work was supported by the Chinese Academy of Sciences, the Natural Science Foundation of China (21373246, 21522309 and 21503242), Natural Science Foundation of Jiangsu Province (BK20130354), Suzhou Science and Technology Projects (SYG201518 and SYG201519).

Appendix A. Supplementary data

Supplementary data associated with this article can be found, in the online version, at http://dx.doi.org/10.1016/j.apcatb.2016.02.026.

References

[1] I. Sádaba, M.L. Granados, A. Riisagerc, E. Taarning, Green Chem. 17 (2015) 4133–4145.
[2] X.L. Du, L. He, S. Zhao, Y.M. Liu, Y. Cao, H.Y. He, K.N. Fan, Angew. Chem. Int. Ed. 50 (2011) 7815–7819.
[3] R. Palkovits, Angew. Chem. Int. Ed. 49 (2010) 4336–4338.

[4] J.J. Bozell, Science 329 (2010) 522–523.
[5] J.P. Lange, R. Price, P.M. Ayoub, J. Louis, L. Petrus, L. Clarke, H. Gosselink, Angew. Chem. Int. Ed. 49 (2010) 4479–4483.
[6] W.H. Luo, U. Deka, A.M. Beale, E.R.H. van Eck, P.C.A. Bruijnincx, B.M. Weckhuysen, J. Catal. 301 (2013) 175–186.
[7] T. Pan, J. Deng, Q. Xu, Y. Xu, Q.X. Guo, Y. Fu, Green Chem. 15 (2013) 2967–2974.
[8] J.C. Serrano-Ruiz, D. Wang, J.A. Dumesic, Green Chem. 12 (2010) 574–577.
[9] H.N. Phama, Y.J. Pagaín-Torres, J.C. Serrano-Ruiz, D. Wang, J.A. Dumesic, A.K. Datye, Appl. Catal. A 397 (2011) 153–162.
[10] Y.J. Pagaín-Torres, J.M.R. Gallo, D. Wang, H.N. Pham, J.A. Libera, C.L. Marshall, J.W. Elam, A.K. Datye, J.A. Dumesic, ACS Catal. 1 (2011) 1234–1245.
[11] R. Buitrago-Sierra, J.C. Serrano-Ruiz, F. Rodríguez-Reinoso, A. Sepúlveda-Escribano, J.A. Dumesic, Green Chem. 14 (2012) 3318–3324.
[12] K. Yan, T. Lafleur, X. Wu, J.J. Chai, G.S. Wu, X.M. Xie, Chem. Commun. 51 (2015) 6984–6987.
[13] K. Yan, Y.Y. Yang, J.J. Chai, Y.R. Lu, Appl. Catal. B 179 (2015) 292–304.
[14] P. Sun, G. Gao, Z.L. Zhao, C.G. Xia, F.W. Li, ACS Catal. 4 (2014) 4136–4142.
[15] W. Wang, J.G. Chen, L.P. Song, Z.T. Liu, Z.W. Liu, J. Lu, J.L. Xiao, Z.P. Hao, Energy Fuels 27 (2013) 6339–6347.
[16] J.Y. Sun, H.C. Liu, Catal. Today 234 (2014) 75–82.
[17] (a) J.P. Lange, J.Z. Vestering, R.J. Haan, Chem. Commun. 33 (2007) 3488–3490; (b) J.Q. Bond, D.M. Alons, R.M. West, J.A. Dumesic, Langmuir 26 (2010) 16291–16298.
[18] A.G. Gayubo, A. Alonso, B. Valle, A.T. Aguayo, J. Bilbao, AIChE J. 58 (2012) 526–537.
[19] A.G. Gayubo, A. Alonso, B. Valle, A.T. Aguayo, J. Bilbao, Appl. Catal. B 97 (2010) 299–306.
[20] J. Vicente, A.G. Gayubo, J. Ereña, A.T. Aguayo, M. Olazar, J. Bilbao, Appl. Catal. B 130–131 (2013) 73–83.
[21] R. Otomo, T. Yokoi, T. Tatsumi, Appl. Catal. A 505 (2015) 28–35.
[22] P. Lanzafame, K. Barbera, S. Perathoner, G. Centi, A. Aloise, M. Migliori, A. Macario, J.B. Nagy, G. Giordano, J. Catal. 330 (2015) 558–568.
[23] S.M.T. Almutairi, B. Mezari, E.A. Pidko, P.C.M.M. Magusin, E.J.M. Hensen, J. Catal. 307 (2013) 194–203.
[24] A. Vjunov, M.A. Derewinski, J.L. Fulton, D.M. Camaioni, J.A. Lercher, J. Am. Chem. Soc. 137 (2015) 10374–10382.
[25] J.G. Zhang, W.Z. Qian, C.Y. Kong, F. Wei, ACS Catal. 5 (2015) 2982–2988.
[26] C.L. Yu, H.Y. Xu, Q.J. Ge, W.Z. Li, J. Mol. Catal. A: Chem. 266 (2007) 80–87.
[27] Z.P. Han, S.R. Li, F. Jiang, T. Wang, X.B. Ma, J.L. Gong, Nanoscale 6 (2014) 10000–10008.
[28] B.J. O'Neill, D.H.K. Jackson, A.J. Crisci, C.A. Farberow, F. Shi, A.C. Alba-Rubio, J. Lu, P.J. Dietrich, X. Gu, C.L. Marshall, P.C. Stair, J.W. Elam, J.T. Miller, F.H. Ribeiro, P.M. Voyles, J. Greeley, M. Mavrikakis, S.L. Scott, T.F. Kuech, J.A. Dumesic, Angew. Chem. Int. Ed. 52 (2013) 13808–13812.
[29] G.Y. Jiang, L. Zhang, Z. Zhao, X.Y. Zhou, A.J. Duan, C.M. Xu, J.S. Gao, Appl. Catal. B 340 (2008) 176–182.
[30] P.L. Benito, A.G. Gayubo, A.T. Aguayo, M. Olazar, J. Bilbao, Ind. Eng. Chem. Res. 35 (1996) 3991–3998.
[31] J. Yu, R. Wang, S. Ren, X. Sun, C. Chen, Q. Ge, W. Fang, J. Zhang, H. Xu, D.S. Su, ChemCatChem 4 (2012) 1376–1381.
[32] M.V.N. Martín, E. Lima, G. Espinosa, Ind. Eng. Chem. Res. 43 (2004) 1206–1210.
[33] M. Larsson, M. Hultén, E.A. Blekkan, B. Andersson, J. Catal. 164 (1996) 44–53.
[34] Q. Li, Z. Sui, X. Zhou, Y. Zhu, J. Zhou, D. Chen, Top. Catal. 54 (2011) 888–896.
[35] S.I. Sanchez, M.D. Moser, S.A. Bradley, ACS Catal. 4 (2014) 220–228.
[36] F.F. Madeira, H. Vezin, N.S. Gnep, P. Magnoux, S. Maury, N. Cadran, ACS Catal. 1 (2011) 417–424.